Ultrafast Excited State Deactivation of Triphenylmethane Dyes†

Yutaka Nagasawa, Yoshito Ando, Daisuke Kataoka, Hirohisa Matsuda, Hiroshi Miyasaka, and Tadashi Okada*

Department of Chemistry, Graduate School of Engineering Science, and Research Center for Materials Science at Extreme Conditions, Osaka University Toyonaka, Osaka 560-8531, Japan

Received: June 5, 2001; In Final Form: November 1, 2001

We have carried out ultrafast pump−probe measurement of four TPM dyes, malachite green (MG), brilliant green (BG), crystal violet (CV), and ethyl violet (EV), with a time resolution of 30 fs. The pump−probe signal showed that solvent dependence arose first in the femtosecond time regime, e.g., the decay of *n*-butanol solution was clearly slower than the methanol solution just 50 fs after the initial photoexcitation. The signal decays in a multiexponential manner and the slower components showed stronger linear dependence on the solvent viscosity than did the faster components. We have also carried out temperature-dependent measurement of ethanol solution and calculated the activation energies from the Arrhenius plots of each components. The activation energies and effective volumes were larger for slower decays. The activation energy of the viscosity of ethanol was larger than that of the decay components of TPM dyes. These observations are explained with a combined effect of microviscosity and intramolecular relaxation. The lifetime of the transient absorption appearing at the red edge of the ground state absorption was longer than any of the reported lifetimes of the excited state absorption around 400 nm. Therefore, the red-edge absorption is assigned to the unrelaxed ground state molecule with the twisted phenyl group.

1. Introduction

A large number of studies have been carried out to understand the ultrafast radiationless deactivation mechanism of triphenylmethane (TPM) dyes.[1] The excited state lifetime becomes shorter in less viscous solvents, and it was interpreted that the diffusive rotation of the amino-substituted phenyl ring is involved in the deactivation process.[2,3] This interpretation can be confirmed by comparing the TPM dyes with rhodamine dyes. Rhodamine dye is an analogue of TPM dye with two phenyl rings connected together. For example, a nonfluorescent TPM dye, brilliant green, becomes a strongly fluorescent laser dye, rhodamine B, by connecting two of the amino substituted phenyl rings with an oxygen atom and adding a 2-carboxylate substituent to the free phenyl ring. It was also shown that a rhodamine dye with a free rotating 4-dimethylamino substituted phenyl ring, instead of the usual 2-carboxylate substituted one, was nearly nonfluorescent in fluid solution.[4,5] Recently synthesized tris(dialkylamino)trioxatriangulenium dyes with three phenyl rings fixed together[6] also exhibited strong fluorescence and long excited state lifetimes.[7,8] TPM dyes have drawn extensive attention because they can be the prototypes for models of barrierless chemical reactions in solution, which can be initialized by photoexcitation.

The aim of our study is to understand the viscosity-dependent nature of the deactivation dynamics. We begin with reviewing the time-resolved studies done in the past and try to clarify what is already known about the dynamics of TPM dyes. The list of the observed ultrafast phenomena is as follows.

(1) In our previous paper, ultrafast decay in the order of 100 fs was observed by pump−probe (PP) measurement at 635 nm.[9] Similar ultrafast decay also appeared in the excited state absorption probed at 390 nm and it was slower in DMSO compared to that in aqueous solution.[10] In this paper, we report a similar ultrafast solvent dependence in a series of *n*-alcohol solutions.

(2) Oscillation with frequency of about 226 cm^{-1} and dephasing time less than 500 fs was observed in the PP signal of MG.[11,12] This was caused by impulsive stimulated resonance Raman scattering and was assigned to the ground state breathing mode of the bonds to the central carbon atom characteristic of TPM dyes.[13−15]

(3) The transient absorption of the excited state appearing around 400 nm, shifted to shorter wavelength with time.[4,16−19] This blue shift was solvent dependent, and the rise time at the blue edge was 1.1 ps for crystal violet (CV) in ethanol.[16] It was assigned to the relaxation process from the Franck−Condon (FC) state to the transient excited state by the diffusive rotation of a phenyl ring around the central carbon atom.

(4) Simultaneously with the blue shift of the transient absorption, ground state bleach became stronger and shifted slightly to shorter wavelengths. This was called the "delayed bleach". Martin et al. explained this phenomenon by the overlap between the blue shifting transient absorption and ground state bleach.[4,16−19] On the other hand, Ishikawa et al. observed similar rise of the bleach on the blue side of the ground state absorption when the red side was excited.[20−23] They ascribed this observation to the isomerization in the ground state. This discrepancy will be discussed in detail later.

(5) Stimulated emission decayed faster than the transient absorption.[24,25] It is commonly explained that twisting of the phenyl ring results in reduction of the transition moment. Therefore, the twisted transient state is often called the "dark state". Some people proposed that this state has a charge transfer (CT) character.[4,16,23,26,27] To the best of our knowledge, time dependent dynamic Stokes shifts of the fluorescence of TPM dyes have never been reported.

† Part of the special issue "Noboru Mataga Festschrift".

10.1021/jp012135c CCC: $22.00
Published on Web 01/17/2002

(6) Together with the 400 nm excited state absorption, another transient absorption appeared on the red edge of the ground state bleach after the stimulated emission decayed. This "red-edge absorption" was explained in three different manners. Martin et al. ascribed that this absorption is also due to the twisted excited state.[4,16] Sundström et al. assigned it to a twisted ground state[28] while Robl and Seilmeier assigned it to a vibrationally hot ground state.[29] The results shown in this paper support the idea of Sundström et al. that the red-edge absorption is due to the twisted ground state.

Summarizing the observations results in following dynamical picture. After the photoexcitation, the initially formed FC state relaxes to a nonfluorescent transient excited state by the diffusional rotation of a phenyl ring. Some people proposed that this dark state is a CT state. Meanwhile, isomerization in the ground state may take place in the same time scale. The dark excited state becomes a vibrationally hot or twisted ground state, and final relaxation takes place in the ground state. Some proposed that the hot or twisted ground state can be observed, while others proposed that they cannot be observed because of the fast relaxation in the ground state.

There are three major theoretical models, which were developed specifically to describe the dynamics of TPM dyes. However, one of them, proposed by Förster and Hoffmann, is now considered to be inappropriate, because it predicts excited state decay of $P(t) = \exp(-\alpha t^3)$ which has never been observed.[3] The model proposed by Bagchi, Fleming, and Oxtoby (BFO) considers a "sink" with a certain functional form at the bottom of the excited state potential surface.[30,31] The initial population caused by photoexcitation spreads diffusively on the excited state potential surface and returns to the ground state through the sink. They have only obtained an analytical solution for the "pinhole" sink, although they have also numerically considered sink functions such as Gaussian and Lorentzian. Another theoretical model proposed by Oster and Nishijima assumes a flat excited state potential that allows the population to freely diffuse to either side.[2] When the population reaches a certain distance from the initial position, it falls off the excited state surface and returns to the ground state. Ben-Amotz et al. generalized this theory and applied it to their experimental observations.[32−34] They concluded that this theory reproduced the experimental results better than did the BFO model.

In this paper, examination of the previously reported results and proposed models is carried out according to our new ultrafast PP measurements with time resolution of 30 fs. Then we discuss the viscosity dependent aspects of the dynamics. Our major interest is to understand the difference between bulk viscosity and microscopic viscosity, which a molecule actually feels. Due to the complexity of our observation, simulations based on theoretical model were not carried out.

2. Experimental Section

The details of the homemade cavity-dumped Kerr lens mode-locked Cr: forsterite laser and pump−probe (PP) measurement system were reported elsewhere.[35] The repetition rate of the cavity-dumping was 100 kHz, and the output was focused into a 4 mm LBO crystal to generate the second harmonic centered at 635−640 nm. The second harmonic pulse energy was 3 to 6 nJ. The autocorrelation trace of the second harmonic pulse was measured by a 0.3 mm BBO crystal with the same setup used for the PP experiment. Gaussian function was assumed for the calculation of the pulse width. The fwhm of the pulse was 30−35 fs when the laser was pumped by a diode-pumped Nd: vanadate laser (Coherent Compass) with CW power of 8 W. When the CW laser was changed to Spectra Physics Millenia IR, the pulse width shortened to 25−28 fs and only 6 W pumping power was necessary to obtain similar output power. To our knowledge, this is the shortest pulse ever generated from a cavity-dumped Cr:forsterite laser. A 25−28 fs pulse was used for the measurement of the D_2O sample. Other experiments were done by 30−35 fs pulse.

The second harmonic pulse was divided into pump and probe pulses by a 50% beam splitter. The energy of the pump pulse was 0.6−0.8 nJ and that of the probe pulse was reduced to 60−80 pJ by an ND filter. The pulses were focused into the sample by 5 or 10 cm focusing lens. The PP measurements were carried out at a magic angle configuration, and the signal was detected by a photodiode and a lock-in amplifier. The optical path of the sample cell was 0.4−0.5 mm, and the optical density of the sample was 0.8−1.2 at the peak. The decay of the signal of TPM dyes did not show any probe pulse energy dependence from 0.8 nJ to 0.2 nJ. For the solvent dependent measurement of MG and BG, the sample solution was circulated in a flow cell to avoid optical damage, and a high-speed silicon detector (DET110) from Thorlabs was used for detection. For other experiments, a homemade high-speed rotational cell and a large-area photoreceiver (Model 2031) from New Focus were used, which resulted in better S/N ratio.

Measurement of the transient absorption at 477 nm was carried out using a dual OPA femtosecond laser system based on a Ti:sapphire laser. The details of the system will be described elsewhere.[36] Briefly, the output of a femtosecond Ti: sapphire laser pumped by SHG of cw Nd^{3+}:YVO_4 laser was regeneratively amplified with 1 kHz repetition rate. The amplified pulse (1 mJ/pulse energy and 85 fs fwhm) was divided into two pulses with same energy. These pulses are guided into two OPA systems, respectively. OPA output pulses are independently converted to the SHG, THG, or FHG. The 635 nm light pulse is provided as SHG of the signal light with 5 mW output power and used as the pump pulse. On the other hand, 477 nm light was produced as FHG of the idler and the output energy of 2 mW, of which intensity was reduced to $<1/5000$ and used as a probe pulse. The pulse duration at the sample position was estimated to be 160 fs from the cross correlation trace at the same position. The intensity of the light monitoring the sample excited with a pump pulse was detected by a photodiode and sent to the microcomputer for further analysis.

Brilliant green (BG), crystal violet (CV), ethyl violet (EV), and malachite green (MG) were purchased from Tokyo Chemical Industry, Aldrich, and Exciton. The counterions for CV and EV were both chloride anion, and those for MG and BG were oxalate and sulfate anion, respectively. Organic solvents were from Kanto and Wako Chemicals and used after distillation when the purity was lower than 99.5%. NMR grade ($>99.75\%$) D_2O was purchased from Wako Chemicals, and water was used after filtering by ion-exchange resin. Absorption and fluorescence spectra were measured by a Hitachi U-3500 spectrophotometer and 850E fluorescence spectrophotometer, respectively.

3. Results

(a) Absorption and Fluorescence Spectra. Molecular structures of TPM dyes are shown in Scheme 1. Three phenyl rings are all amino-substituted for D_3 symmetric dyes, CV and EV, while one is not substituted for C_2 symmetric dyes, MG, and BG. The absorption spectra of TPM dyes in ethanol are shown in Figure 1 along with the laser spectrum. The absorption peaks of TPM dyes showed a slight red shift when the alkyl chain of *n*-alcohol elongated. The peak shifted from 619 to 624

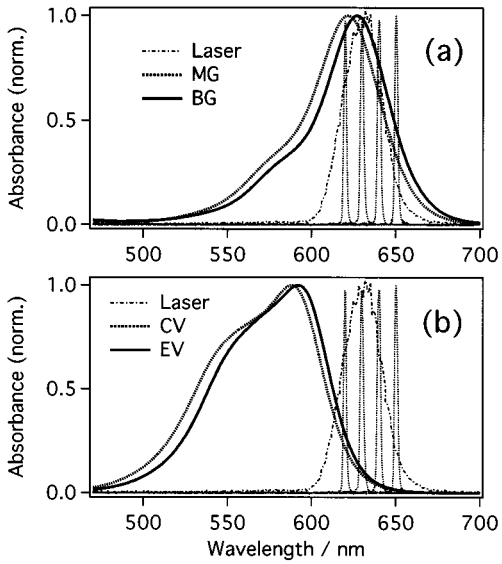

Figure 1. Absorption spectra of (a) MG and BG, and (b) CV and EV in ethanol solution. Laser spectrum is also shown for comparison. The probe beam was detected with and without a monochromator. The wavelength resolved spectra at 620, 630, 640, and 650 nm are also shown.

SCHEME 1: Structures of C_2 Symmetric TPM Dyes, e.g., Malachite Green (MG) and Brilliant Green (BG), and D_3 Symmetric Dyes, e.g., Crystal Violet (CV) and Ethyl Violet (EV)

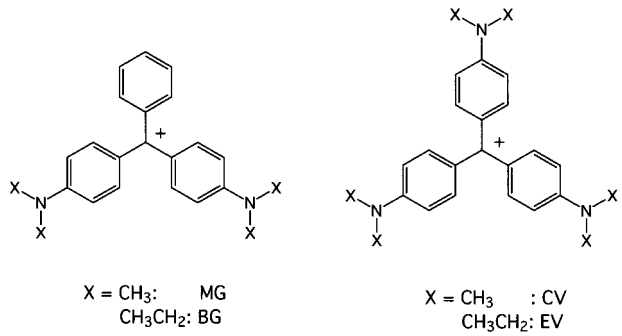

nm for MG when the solvent was changed from methanol to *n*-butanol, while the peak of CV shifted from 587 to 590 nm. The Stokes shifts between the absorption and fluorescence peaks were 670 and 310 cm^{-1} for MG and CV in ethanol, respectively. These values are smaller than that of rhodamine dyes and much smaller than that of coumarin dyes, i.e., 880 and 4770 cm^{-1} for rhodamine 6G and coumarin 153 in ethanol, respectively. The reorganization energies are roughly half of the values of the Stokes shift. Thus, the charge shift upon photoexcitation seems to be relatively small for TPM dyes, although these small Stokes shifts can be partially due to the short excited lifetime. Since the excited state lifetimes of TPM dyes are extremely short, the molecule may return to the ground state before the solvation process completes on the excited state.

In the absorption spectra of CV and EV, a strong shoulder appeared on the blue side, which has been a subject of debate for many years.[1,22,37−46] There are two prevailing theories for the appearance of the shoulder: that there are two isomers in equilibrium,[37,40−42] and that desymmetrization gives rise to two excited states.[38,39,43,46] Recently, from their transient hole-burning experiment, Ishikawa et al. explained that it was due to a ground state conformer with a solvent induced pyramidal C_3 symmetric structure.[20,22] However, Lovell et al. argued that such pyramidal conformer is not responsible because a similar shoulder also appeared in the absorption spectrum of planner tris(dialkylamino)trioxatriangulenium dye[6] with three phenyl rings fixed together.[45] They advocated the model first suggested by McHale et al.,[46] that a dipole or a counteranion interacting with dimethylamino group reduce the symmetry and split both the ground and the excited states of TPM dyes. If the isomer in the ground state reduces the symmetry, it will result as a splitting of the degenerated excited state. Therefore, these two effects cannot be discussed separately. The reduction of the symmetry can be caused either by ion pairing, twisting of the phenyl ring, or by dye aggregation.[1] Since the lower symmetry of MG and BG, the excited states split widely and new absorption appears around 430 nm for these dyes.[1] Thus, the weak shoulders appearing in the absorption spectra of C_2 symmetric dyes are most likely vibrational structure. However, Ishikawa et al. suggested three isomers or inhomogeneity in the ground state of MG and BG.[23] The discussion on the ground state conformer or inhomogeneity will be continued later.

Figure 1 shows that the femtosecond pulse excites slightly on the red side of the peak absorption for C_2 symmetric dyes, while it excites the red edge of the absorption for D_3 symmetric dyes. Thus contribution of stimulated emission to the measured PP signal should be stronger for D_3 symmetric dyes. The probe pulse was detected with and without a monochromator after transmitting through the sample cell. The wavelength resolved spectra of the probe beam are also shown in Figure 1. The center wavelengths were 620, 630, 640, and 650 nm with fwhm of about 3 nm. The wavelength resolved signal at 640 and 650 nm for CV and EV should be dominated by stimulated emission.

(b) Pump−Probe Measurement. PP signals are generally expressed in terms of transmission difference, ΔT,, or absorption difference, ΔAbs. When it is expressed in terms of ΔT,, increase of transmission emerges as a positive signal and increase of absorption emerges as negative signal, while it is the opposite in the case of ΔAbs. Our experiments are expressed in terms of ΔT,, except the measurement at 477 nm. ΔT is equivalent to ΔAbs only if the signals are very small. This approximation is valid because the ΔAbs is less than 10^{-3} for our experimental condition. PP signals of TPM dyes in series of hydrogen bonding solvents are shown in Figure 2. For D_3 symmetric dyes, CV, and EV, measurement in aqueous solution was not carried out because of their strong tendency to form aggregates in water.[47] At time origin, the dye molecules are excited by the pump beam, which causes a sudden increase of ΔT. Ground state bleach and stimulated emission are both responsible for the positive signal. Recovery of the thermally equilibrated ground state causes the signal to return gradually to zero. The decay of the signal was slower in longer alcohols as expected from the viscosity dependence. TMP dyes with larger amino group decayed slower in all solvents, which confirms the previous studies.[26−28] Every signal showed oscillations caused by impulsive stimulated resonance Raman scattering. For C_2 symmetric dyes, MG and BG, after the initial ultrafast decay, the decay slows down and forms a plateau and then continues to decay multiexponentially. The D_3 symmetric dyes also decayed multiexponentially, but no plateau was observed. The fitting of the signal decay was carried out by convoluting the autocorrelation trace with a fitting function, $f(t)$, which is a sum of exponential functions and exponentially damped cosine functions,

$$f(t) = \sum_i A_i \exp(-t/\tau_i) + \sum_j A_j \exp(-t/\tau_j)\cos(\nu_j t + \phi_j) \quad (1)$$

where A_i is the intensity, τ_i is the lifetime or the dephasing time, and ϕ_i is the phase. To avoid any prejudice, we did not assume

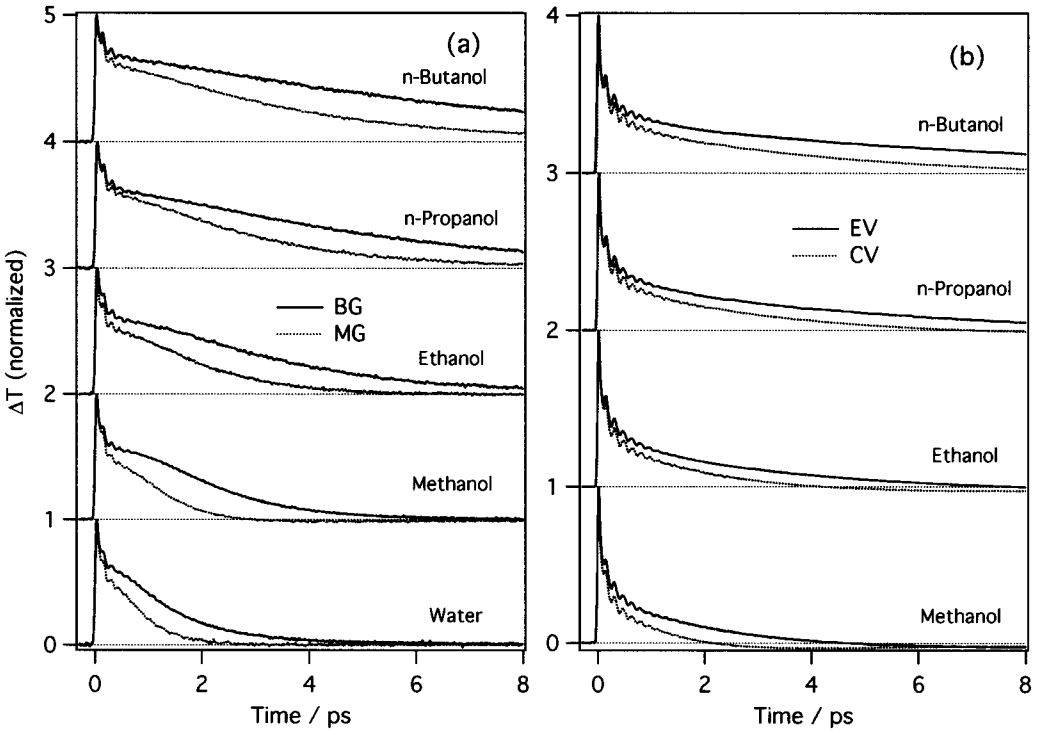

Figure 2. Transient transmission signals of (a) MG and BG, (b) CV and EV in valious hydrogen bonding solvents pumped and probed at 635 nm.

TABLE 1: Fitting Parameters Obtained from the Convolution Fitting of CV Solutions[a]

	methanol	ethanol	*n*-propanol	*n*-butanol
τ_1/ps	0.017	0.037	0.062	0.075
(A_1)	(0.54)	(0.43)	(0.41)	(0.42)
τ_2/ps	0.12	0.20	0.29	0.39
(A_2)	(0.23)	(0.23)	(0.20)	(0.17)
τ_3/ps	1.3	2.4	3.4	4.6
(A_3)	(0.23)	(0.31)	(0.30)	(0.30)
T_{rise}/ps	4.1	6.0	12.0	18.0
(A_{rise})	(−0.07)	(−0.11)	(−0.07)	(−0.05)
ν_1/cm^{-1}	204	204	206	207
$\tau_{\nu 1}$/ps	0.39	0.36	0.37	0.37
($A_{\nu 1}$)	(0.05)	(0.09)	(0.11)	(0.12)
ν_2/cm^{-1}	425	425	425	425
$\tau_{\nu 2}$/ps	0.12	0.10	0.10	0.11
($A_{\nu 2}$)	(0.01)	(0.03)	(0.03)	(0.02)
ν_3/cm^{-1}	445	445	445	445
$\tau_{\nu 3}$/ps	1.20	1.04	1.38	1.29
($A_{\nu 3}$)	(0.01)	(0.02)	(0.02)	(0.02)
λ_{abs}/nm	587	588	589	590
λ_{flu}/nm	597	600	597	601
η/cP	0.6	1.2	2.2	2.9

[a] A_{1-3} and τ_{1-3} are amplitudes and time constants for the positive components, and A_{Rise} and τ_{Rise} are for the negative one, respectively. ν_{1-3}, $\tau_{\nu 1-3}$, and $A_{\nu 1-3}$ are frequencies, dephasing times, and amplitudes for the oscillatory components. Frequencies of 425 and 445 cm^{-1} were fixed during the fitting. Solvent viscosity, η, absorption, λ_{abs}, and fluorescence maxima, λ_{flu}, are also shown. Amplitudes are normalized in a manner to be 1 when all the components are added, including the negative one.

TABLE 2: Fitting Parameters Obtained from the Convolution Fitting of EV Solutions[a]

	methanol	ethanol	*n*-propanol	*n*-butanol
τ_1/ps	0.021	0.033	0.039	0.064
(A_1)	(0.52)	(0.44)	(0.43)	(0.31)
τ_2/ps	0.21	0.30	0.35	0.47
(A_2)	(0.20)	(0.20)	(0.19)	(0.18)
τ_3/ps	2.7	3.9	5.9	9.9
(A_3)	(0.27)	(0.26)	(0.26)	(0.28)
τ_{rise}/ps	5.8	11.3	20.5	24.5
(A_{rise})	(−0.11)	(−0.07)	(−0.05)	(−0.03)
ν_1/cm^{-1}	208	207	208	210
$\tau_{\nu 1}$/ps	0.37	0.32	0.29	0.27
($A_{\nu 1}$)	(0.06)	(0.08)	(0.10)	(0.13)
ν_2/cm^{-1}	445	445	445	445
$\tau_{\nu 2}$/ps	0.11	0.15	0.20	0.12
($A_{\nu 2}$)	(0.06)	(0.09)	(0.07)	(0.13)
λ_{abs}/nm	590	592	593	594

[a] A_{1-3} and τ_{1-3} are amplitudes and time constants for the positive components, and A_{rise} and τ_{rise} are for the negative one, respectively. ν_{1-3}, $\tau_{\nu 1,\ \nu 2}$, and $A_{\nu 1,\ \nu 2}$ are frequencies, dephasing times, and amplitudes for the oscillatory components. Frequency of 445 cm^{-1} was fixed during the fitting. Absorption maximum, λ_{abs}, is also shown. Amplitudes are normalized in a manner to be 1 when all the components are added, including the negative one.

any kinetic model to construct the fitting function. Both positive and negative intensities were necessary to fit the data. The results of the fitting for the C_2 symmetric dyes were listed in our previous paper.[9,48] The results for the D_3 symmetric dyes are listed in Table 1 and Table 2. The viscosity dependence of the decay components is shown in Figures 11 and 12 and will be discussed later.

The initial part of the PP signal for CV in n-alcohols is shown in Figure 3. It can be seen that the solvent dependence manifests itself in a very early time scale. The decay in *n*-butanol and methanol can be already distinguished at 50 fs. The PP signals of MG in aqueous solution and in D_2O are compared in Figure 4. In this case the ultrafast part of the signal completely overlaps, despite the difference in the slower part. The rise times needed to fit the plateau were 218 and 224 fs for water and D_2O, respectively, which are only slightly different. The time constants for the second decay components were 435 and 570 fs, for water and D_2O, respectively. The inset of Figure 4 shows that not only the decay of the positive part but also the decay of the negative part slowed. The lifetimes of the negative components were 4.2 and 6.0 ps for water and D_2O, respectively.

The decay of the D_3 symmetric dyes all had negative components with long lifetimes, which means manifestation of

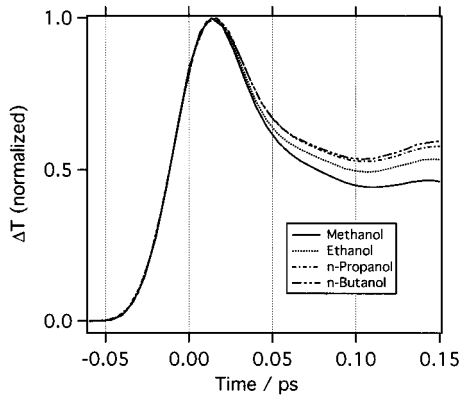

Figure 3. Initial ultrafast part of the transient transmission signals of CV in *n*-alcohol solvents pumped and probed at 635 nm.

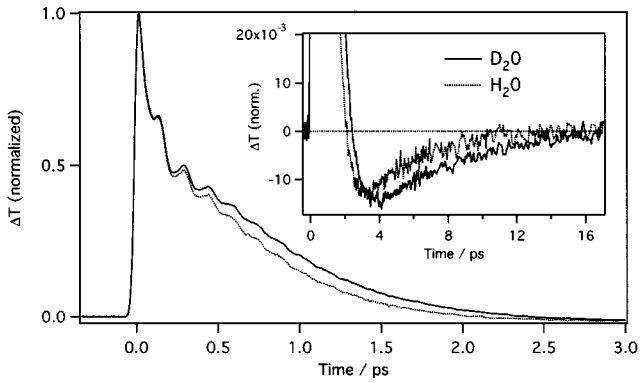

Figure 4. Transient transmission signals of MG in water and in D_2O pumped and probed at 635 nm. Inset shows the magnification of the negative part.

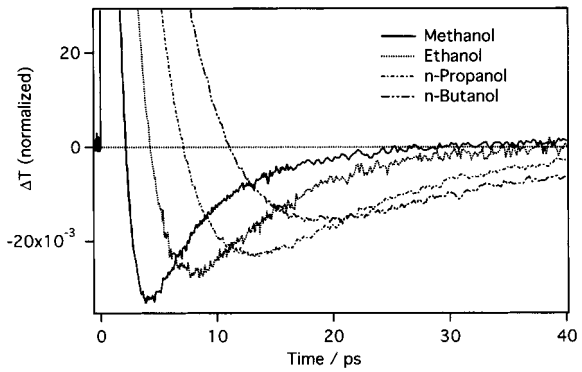

Figure 5. Magnification of the negative part of the transient transmission signals of CV in *n*-alcohol solvents pumped and probed at 635 nm.

transient absorption. The negative part of the PP signals for CV is magnified in Figure 5. It can be seen that the lifetime of the negative component also gets longer in longer *n*-alcohols. For MG in water and methanol, negative component was also observed although the intensity was extremely weak. When the probe beam was wavelength resolved, negative signal appeared at longer wavelengths. Figure 6 shows probe wavelength resolved PP signals for MG and CV in methanol. The signals of MG in methanol show that the negative signal can be seen only at 640 and 650 nm. It can be also seen that the plateau appears only in shorter wavelengths. Wavelength-resolved signals of CV in methanol showed no plateau at shorter wavelengths, and all signals had a negative part. The signal without wavelength resolution detects the average of these signals weighted by the laser spectrum and extinction coefficient.

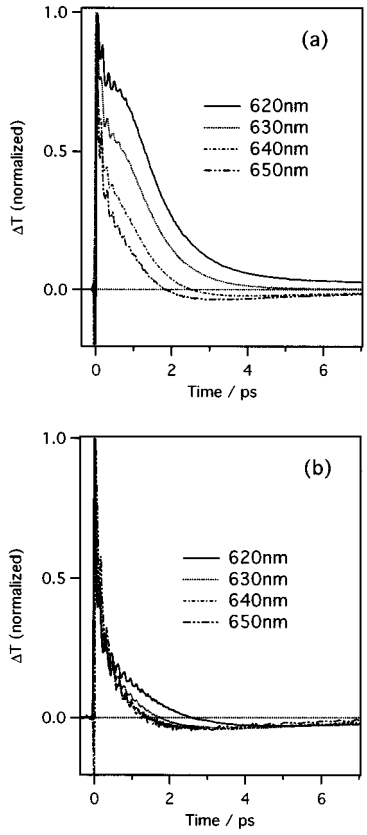

Figure 6. Probe wavelength resolved transient transmission signals of (a) MG and (b) CV in methanol.

The amplitudes of the Fourier transformed spectra of the wavelength-resolved signals are shown in Figure 7. The spectra are dominated by the mode at 210−230 cm^{-1} characteristic of TPM dye[12−14,45,46,49−51] and vibrations with frequency as high as 440−470 cm^{-1} can be seen. The intensity of the 440−470 cm^{-1} bands was stronger when detected at both edges of the laser spectrum. It is well known that the intensities of higher frequency modes become stronger when probe beam is wavelength resolved and the signal is detected further from the center of the laser spectrum.[52]

Transient absorption signals for MG and CV in methanol probed at 477 nm are shown in Figure 8. Since ΔAbs is detected in this measurement, transient absorption appears as a positive signal. The probe wavelength was chosen to avoid the ground state absorption of MG. Rise with a time constant of 0.56 ps was detected in the MG signal while only decay can be seen for CV. The lifetime of the excited state was obtained to be 0.70 and 1.67 ps for MG and CV, respectively. Anisotropy decays of MG and CV in methanol are shown in Figure 9.

The decays of MG and CV in ethanol became slower at lower temperatures as shown in Figure 10. Below the melting point at 158 K, the sample became opaque and PP measurement was not possible. However, rapid cooling resulted in plastic phase transition, and PP measurement was possible at 100 K. The decay time constant of the initial ultrafast decay was almost temperature insensitive and it manifested itself even at 100 K. Arrhenius plots of the decay components are shown in Figure 13.

4. Discussion

(a) Origin of the Ultrafast Solvent Dependent Decay. The solvent dependence manifests itself already in the initial part of the PP signal as shown in Figure 3. The decay in *n*-butanol

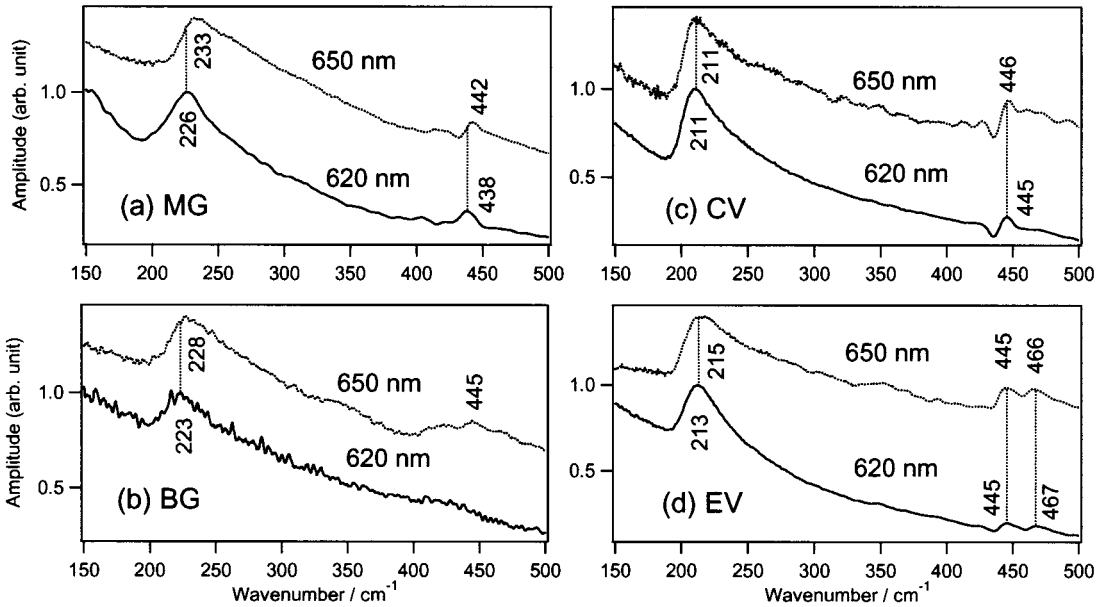

Figure 7. Amplitude of the Fourier transform spectra of the signals of (a) MG, (b) BG, (c) CV, and (d) EV in methanol solution probed at 620 and 650 nm.

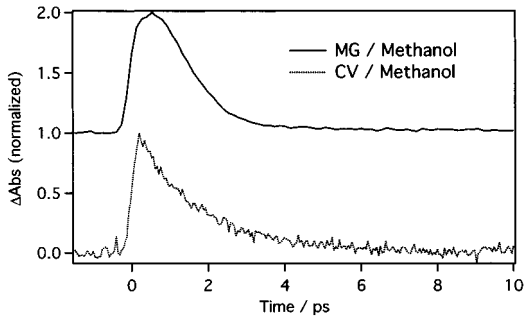

Figure 8. Transient absorption signals of (a) MG and (b) CV in methanol probed at 477 nm and pumped at 635 nm. The signal is represented in terms of absorption difference, ΔAbs.

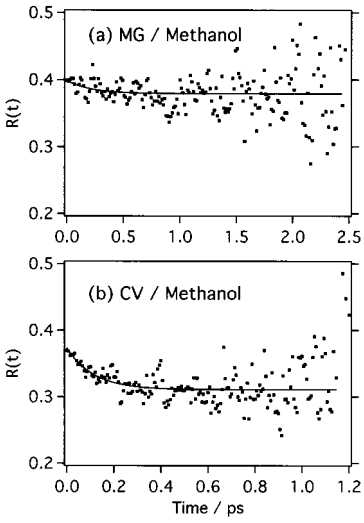

Figure 9. Anisotropy decays of (a) MG and (b) CV in methanol solution. Dots are the experimental results and the curves are the fitting results of the signal.

and methanol can be already distinguished at 50 fs. The time constant for the fastest decay, τ_1, for CV and EV gradually increases from 17 to 75 fs and from 21 to 64 fs, respectively, as the *n*-alcohol chain elongates (Table 1 and Table 2). Although these results are very close to our limit of time resolution, such

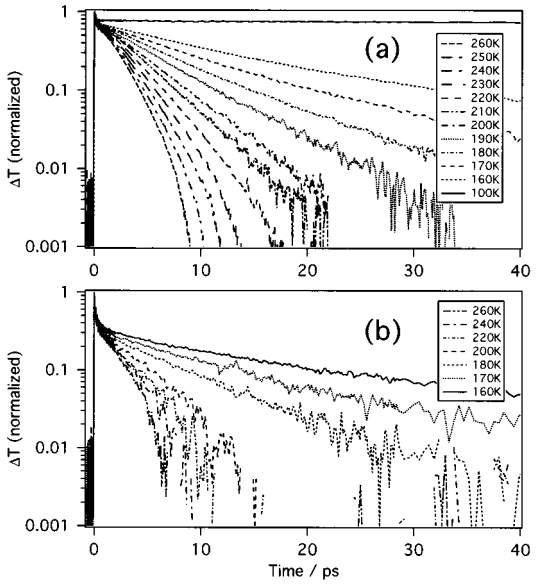

Figure 10. Temperature dependence of transient transmission signals of (a) MG and (b) CV in ethanol pumped and probed at 635 nm.

a systematic difference is remarkable. Mokhtari et al. observed similar ultrafast decay in the excited state absorption probed at 390 nm.[10] The time constants of 30−50 fs and 50−80 fs for MG and CV, respectively, in water increased to roughly 120 and 180 fs in dimethyl sulfoxide. Although, these authors avoided elaborate discussion, they attributed the ultrafast decay as originating from the relaxation of solvent-perturbed intramolecular low frequency modes. Another possibility that they have ignored is the inertial solvation process. Inertial solvation is the ultrafast process that occurs within 100 fs, which is thought to be caused by small angle free rotation of a few solvent molecules within the first solvation shell.[53,54]

Since there is a possibility that inertial solvation in alcohols and water can proceed via librational motion of the −OH group, comparison of MG signals in water and in D_2O was carried out. The results in Figure 4 show that the initial part overlapped completely, while there is a difference in the slower part. Similar results were reported for the study of the solvation process of

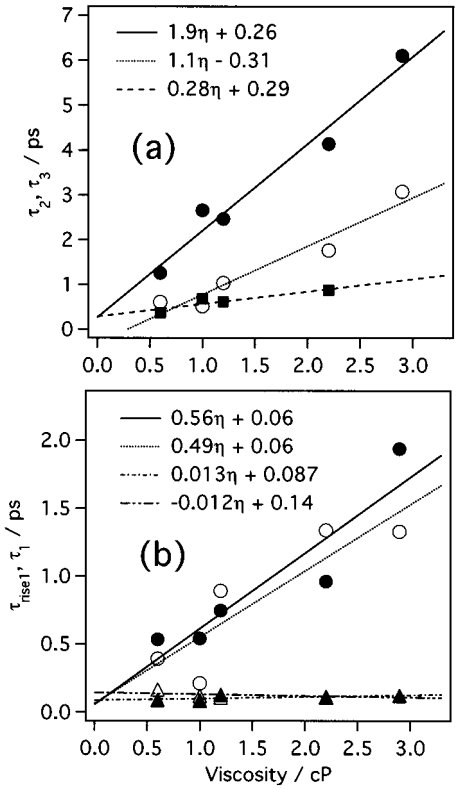

Figure 11. (a) Viscosity dependence of the time constants τ_2 and τ_3 of BG (■ and ●, respectively) and τ_3 of MG (○). (b) Viscosity dependence of the time constants τ_1 and τ_{rise1} of BG (▲ and ●, respectively) and MG (△ and ○, respectively).

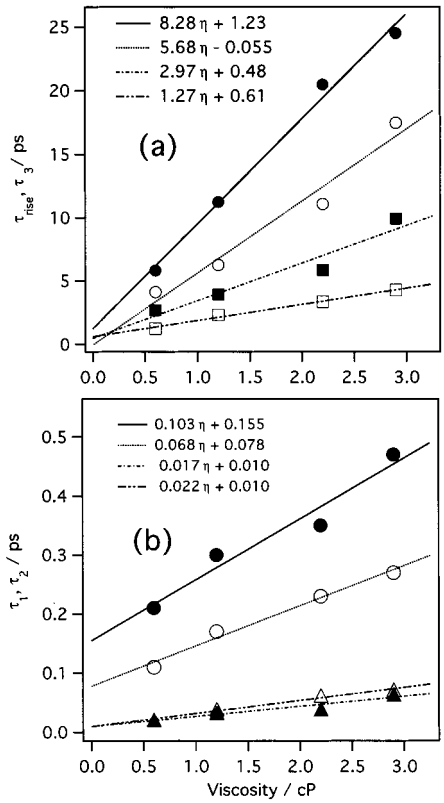

Figure 12. (a) Viscosity dependence of the time constants τ_3 and τ_{rise} of EV (■ and ●, respectively) and CV (□ and ○, respectively). (b) Viscosity dependence of the time constants τ_1 and τ_{rise1} of EV (▲ and ●, respectively) and CV (△ and ○, respectively).

a xanthene dye, LD690, by a three-pulse photon echo experiment.[55,56] Slowing down of the echo decay with increasing alcohol chain length was observed, while no discernible difference was observed between normal and deuterated methanol signals. We conclude that the ultrafast part of the decay is indeed solvent dependent, although no effect of increased mass by the deuteration was observed. This could be due to the fact that the ultrafast decay is not affected by the libration of the −OH group or that such an effect is too minor to detect. The difference in the slower part can be the effect of viscosities, which are 1.002 cP and 1.248 cP at 20 °C for water and D_2O, respectively. This effect will be discussed again later.

(b) Origin of the Plateau Observed in the MG and BG Signals. After the initial ultrafast decay, the decay slowed and formed a plateau for C_2 symmetric dyes, MG and BG, as can be seen in Figure 2a. A rise component was necessary to fit the plateau,[9,48] and the rise time matched that obtained for the rise of the excited state absorption. It is known that the diffusive twisting of the phenyl ring in the excited state causes the blue shift of the excited state absorption. Thus, delayed rise can be observed when the excited state absorption is detected on the blue side. We have obtained a rise time of 0.21 ps at 635 nm while Mokhtari et al. obtained 0.27 fs at 390 nm for MG in water.[10] Therefore, it can be concluded that the plateau originates from the excited state dynamics. The plateau became an apparent rise when transient dichroism was detected at 610 nm.[57] Transient absorption measurement showed that the ground state bleach of TPM dyes became stronger and shifted slightly to shorter wavelengths.[4,16−19] This was called the "delayed bleach". Such an increase of bleach can be hardly explained from the viewpoints of transient hole-burning, because the hole must be the deepest at time origin for a usual harmonic potential surface. Therefore, Martin et al. explained this phenomenon in terms of overlap between the blue shifting transient absorption and ground state bleach.

On the other hand, Ishikawa et al. observed a similar rise of the bleach on the blue side of the ground state absorption when the red side was excited.[20−23] The rise time they have obtained was solvent independent with a constant value of about 500 fs. They ascribed this observation to the isomerization in the ground state, because the shape of the hole depended on excitation wavelength. However, according to the BFO model,[30,31] the ground state recovery can depend on excitation wavelength, since the position of the initial excited state population depends on excitation energy. If the initial population is generated far from the "sink", ground state recovery will be delayed while no such delay will appear when it is close to the sink. Ishikawa et al. tried to overcome this difficulty by establishing a kinetic model that considers both the delayed rise of the bleach and excited state relaxation. However, they never considered the possibility of the excited state absorption overlapping with that of the ground state. If such an overlap is present, it will affect the dynamics of the hole and two photon absorption could also happen with high power excitation.

Jonas and Fleming have tried to explain the delayed bleach by considering two emitting excited states.[58] If the initially excited state has smaller transition moment than the relaxed excited state, it will eventually cause a delayed increase of stimulated emission. However, the contribution of the stimulated emission should be dominant on the red side of the ground state absorption and not on the blue. Moreover, the relaxed excited state of TPM dyes is generally considered to have a smaller transition moment than the initial state. Du et al. ascribed the rise observed in the transient dichroism to a low frequency oscillation.[57] However, due to the strong viscosity dependence,

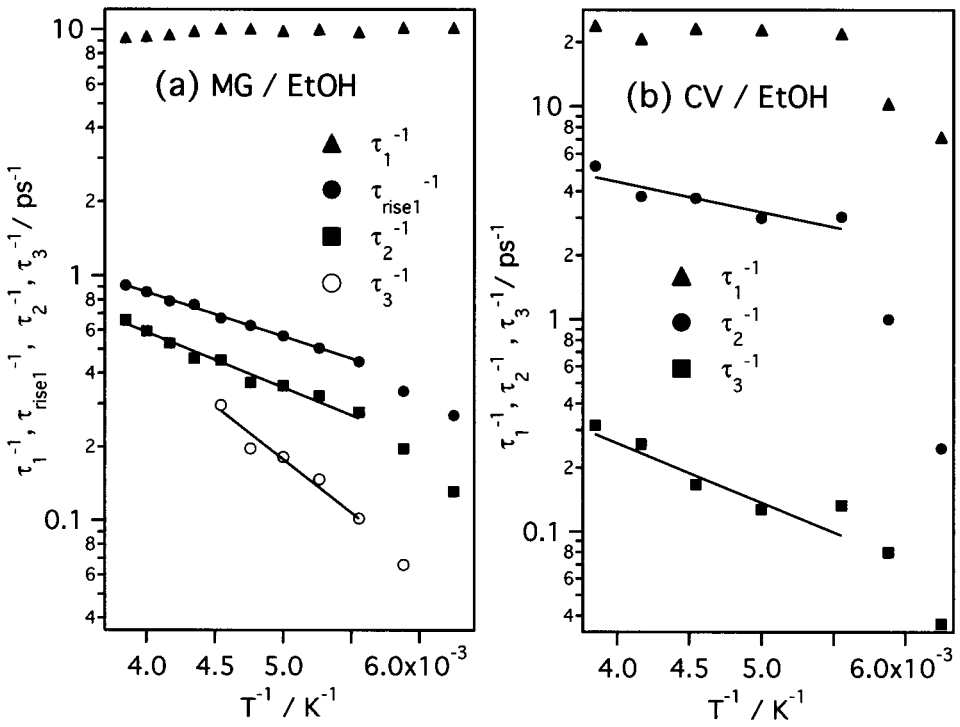

Figure 13. (a) Arrhenius plots of the time constants τ_1, τ_{rise1}, τ_2, and τ_3 of MG in ethanol solution (▲, ●, ■, and ○, respectively). (b) Arrhenius plots of the time constants τ_1, τ_2, and τ_3 of CV in ethanol solution (▲, ●, and ■, respectively). Fittings were carried out above 180 K.

the rise seems to be a diffusive process rather than a damped oscillation. Thus, these models seem to be inadequate for TPM dyes.

If the excited state absorption or stimulated emission overlaps with ground state bleach, it may appear in the time-dependent anisotropy measurement. If the S_n-S_1 absorption has different direction of the transition moment compared to that of S_1-S_0 absorption, initial anisotropy may not start from 0.4. Moreover, if the rotation of the phenyl ring changes the direction of the transition moment, anisotropy of stimulated emission should decay simultaneously with the rotation. Therefore, the anisotropy measurement was carried out for MG and CV in methanol (Figure 9). The time-dependent anisotropy of MG in methanol shown in Figure 9a, started from 0.40 and decayed to 0.38 with time constant of 220 fs. This change was so small that it is in the limit of our experimental resolution. However, the anisotropy of CV showed a clear decay from 0.37 to 0.31 with time constant of 110 fs (Figure 9b). This time constant matches with that of the second decay component, τ_2, of CV in methanol, which is 120 fs (Table 1). Since the PP signal of CV is expected to have stronger contribution from the stimulated emission, this result indicates that the rotation of the phenyl ring not only results in decrease of the transition moment but also the rotation of the transition moment. Another explanation is that the anisotropy decay is caused by the thermalization between two closely neighboring excited electronic levels. For D_3 symmetric dyes, two excited states with perpendicular transition moments can be degenerated.[1] For C_2 symmetric dyes, such a effect will not show up because the electronic levels are much widely separated. In case of MG, the excited state absorption may not be overlapped with the ground state bleach within our experimental observation window because the initial anisotropy was 0.40. However, we still consider the origin of the plateau to be the excited state relaxation.

The reason for the plateau to be undetected in the signals of D_3 symmetric dyes is that PP measurement was carried out on the red edge of the ground state absorption. In such a wavelength, stimulated emission will dominate the signal and excited state dynamics will only result in signal decay. This effect can be seen in the probe wavelength resolved experiment of MG in methanol (Figure 6a). The plateau appeared only in shorter wavelengths, while at longer wavelengths, MG signal became similar to that of CV.

For TPM dyes, there are two distinct excited states, the fluorescent initially populated state and the twisted dark state. For D_3 symmetric dyes, there may be a third state because the fluorescent state can be degenerated. For C_2 symmetric dyes, the third state is well separated from the S_1 state and becomes an S_2 state, which absorbs around 430 nm. This S_2 state is known to be also fluorescent.[59] In our experiment, mainly the lower degenerated state was excited for the D_3 symmetric dyes, because the excitation wavelength was set at the red edge of the absorption spectrum. The relaxation process from the initially populated fluorescent state to the twisted dark state has been observed as the blue shift of the transient absorption or the decay of the fluorescence. The twisted dark state seems to be almost completely nonfluorescent, because time dependent red shifts of the fluorescence spectrum have never been observed and the Stokes shift between the absorption and the fluorescence spectra is small for TPM dyes. Since the twisted state is energetically more stable than the fluorescent state, fluorescence from the twisted state should be red shifted. The rapid decline of the fluorescent state contradicts with the model of Oster and Nishijima, which assumes a flat potential surface in the excited state. If the dark state and the fluorescent state occupy the same energy level, fluorescence will not decline completely because a thermal equilibrium will be reached between the two states. However, for MG, the population in the fluorescent state may not vanish completely. The fluorescence lifetime of MG in water measured by the up-conversion technique was 0.54 ps,[59] which is longer then the excited state relaxation time of 200−300 fs. The origin of this long-lived fluorescence cannot be the relaxed twisted state because of the absence of the red shift. We would like to conclude that the potential energy surface of the excited

state may be shallow but not completely flat. The time-resolved fluorescence spectrum of auramin, an analogous dye with only two phenyl rings, was reconstructed from the up-conversion measurement, and it showed only a small red shift.[60,61] The relaxed excited state of auramine is also considered to be nonfluorescent. To the best of our knowledge, time-resolved fluorescence spectrum has never been measured for TPM dyes.

Some researchers proposed that the dark excited state has a CT character despite the weak dependence on dielectric constant.[4,16,23,26,27] Martin et al. once excluded the possibility of twisted intramolecular charge transfer (TICT) model for the dark state[19] because the decay times were similar to each other in ethanol and dioxane, which have similar viscosities, 1.08 cP and 1.09 cP, respectively, while the dielectric constants are significantly different, 24.5 and 2.2, respectively. However, in their later reports,[4,16] they still consider the dark state as a CT state despite the weak dependence on dielectric constant. Since our results neither support nor oppose CT models, we would like to avoid further evaluation. Nevertheless, twisting of the phenyl ring can disturb the delocalized π-electron conjugation and can somewhat result in redistribution of the charge.

(c) Origin of the Negative Signal Observed in the CV and EV Signals. When the probe beam was wavelength resolved by a monochromator, a negative signal appeared in PP signals detected at longer wavelengths for MG and BG. Figure 6a shows the negative signal of MG in methanol detected at 640 and 650 nm. For CV and EV, negative signal appeared without resolving the probe wavelength, because laser wavelength was centered on the red edge of the absorption. The expansions of the negative parts of CV signals are shown in Figure 5. These results indicate that the negative signal is the previously reported transient absorption appearing at the red edge of the ground state bleach.[4,16,25,28,29,32,33,48] There is some opposition about the origin of this transient absorption. Sundström et al. assigned it to a ground state species with a twisted conformation relative to that of the normal dye form.[28] Robl and Seilmeier assigned it to a vibrationally hot ground state and estimated a transient vibrational heating to an internal temperature of 600 K.[29] Martin et al. discarded both possibilities and concluded that the dark excited state has two absorption bands around 380 and 700 nm.[16] They argued that it is not the vibrationally hot ground state because vibrational cooling rate is not expected to depend on the solvent viscosity. They also argued that a transient ground state with a distorted geometry would not be expected to absorb in the red side of the stable ground state that has a nearly flat propeller geometry, since a blue shift is expected when one reduces the π-electron delocalization length of a conjugated system. However, this is not always true because electronic transition energy depends on the energy difference between the two electronic levels and not only to that of the lower one. If the twisted form is not the stable configuration in the ground state while it is in the excited state, the distorted ground state absorbs less energy than the stable ground state. Moreover, even if the vibrational cooling rate does not depend on the solvent viscosity, it should depend on the thermal conductivity of the solvent.[62] Thermal conductivity reduces from 0.181 to 0.131 kcal/(mh °C) when the solvent is changed from methanol to *n*-butanol. There is no reason to discard the origin of the red-edge absorption to be the transient ground state. We would also like to mention that there is no clear distinction between vibrationally hot ground state and twisted ground state. The distribution of the twisted angle should also depend on temperature. At higher temperatures, the distribution will become broader. Thus, the distribution of the twisted angle itself can be the measure of temperature.

We have carried out high accuracy measurement of the decay of the red-edge transient absorption and concluded that the lifetime was longer than any of the reported lifetimes of the excited state absorption around 400 nm. Ben-Amotz et al. reported excited state lifetimes of CV probed at 480 nm as 1.9, 3.5, and 8.8 ps in methanol, ethanol, and *n*-butanol solution, respectively.[25] Martin et al. reported lifetimes of CV measured at 404−407 nm as 3.5, 7.2, and 7.0 ps in ethanol, *n*-propanol, and *n*-butanol solution, respectively.[16] The lifetimes of the red-edge absorption for CV we have measured, which were 4.1, 6.0, 12.0, and 17.9 ps in methanol, ethanol, *n*-propanol, and *n*-butanol solution, respectively, were much longer than any of these measurements. To confirm this observation, we have also carried out measurements probed at 477 nm by ourselves (Figure 8). Obtained excited state lifetimes of MG and CV in methanol were 0.70 and 1.67 ps, respectively, which were both more than twice as short as the lifetime of the red-edge transient absorption, 4.2 and 4.1ps for MG and CV, respectively. These discrepancies are too large to be caused by the difference in experimental conditions. They strongly indicate that the transient absorption bands around 380 and 700 nm originate from different electronic states. When the probe wavelength was resolved, the signal of MG in methanol (Figure 6a) showed that the negative signal with lifetime of 4.2 ps at 650 nm turns into a positive signal with a lifetime of 5.3 ps at 620 nm. Similar phenomena were also observed with other TPM dyes when the probe beam was wavelength resolved. These observations are consistent with the picture of declining vibrationally hot and/or twisted ground state and the repopulation of the equilibrium ground state near the ground state absorption maximum. We conclude that the red-edge transient absorption is due to the twisted ground state, as predicted by Sundström et al. This ground state can also be vibrationally hot, although we think that the twisted conformation is the essence of this transient state because of the strongly viscosity-dependent lifetime.

Since the red-edge absorption has the longest lifetime, the ground state potential surface may be shallow and distribution of conformers may be populated by the thermal fluctuation. This picture is consistent with that of Ishikawa et al.[20−23] and Cremers et al.[63] However, Ishikawa et al. concluded that the thermal equilibration time had a solvent independent constant value of 500 fs, while we observed equilibration in longer time scale with strong solvent viscosity dependence. Some intramolecular vibrational frequencies may depend on the magnitude of the twisting. If broad distribution of conformers is present in the ground state of TPM dyes, a wavelength-dependent resonance Raman scattering experiment has a potential to detect such dependence. As an alternative, we have carried out Fourier transform of the wavelength resolved PP signal (Figure 7). The frequencies of CV and EV showed almost no wavelength dependence, while those of MG and BG showed slight dependence. Figure 7 shows that, when the probe wavelength was changed from 620 to 650 nm, the breathing mode of MG and BG shifted from 226 to 233 cm^{-1} and from 223 to 228 cm^{-1}, respectively. The difference was only 5−6 cm^{-1}, which is almost at the limit of our experimental resolution, although it seemed to be reproducible. Fitting of the PP signal by exponentially damped cosine function resulted in similar dependence, the frequency changed from 215 to 231 cm^{-1} for MG in methanol when the wavelength was changed from 620 to 650 nm, while that of CV in methanol was constant at 205 cm^{-1}. The reason there is no dependence for CV may be that

only one conformer was detected since the probe beam was centered near the red edge of the ground state absorption. To the best of our knowledge, there is no report on profiling the excitation wavelength dependence of resonance Raman spectrum of TPM dyes. There is only one study in the literature that reports the comparison of the Raman spectrum at two different wavelengths.[14] The frequency of MG in aqueous solution shifted from 230 to 235 cm^{-1} when the wavelength was changed from 441.6 to 632.8 nm. These results may indicate an inhomogeneous ground state, although we would not further elaborate on this idea since the frequency difference was so small.

(d) Viscosity and Temperature Dependences. To investigate the viscosity dependence on PP signal, we have carried out a convolution fitting analysis. For C_2 symmetric dyes, three components with positive amplitude, $\tau_1-\tau_3$, and two components with negative amplitude, τ_{rise1} and τ_{rise2}, were necessary at maximum. The component τ_{rise1} was necessary to reproduce the plateau of the signal, while τ_{rise2} was the lifetime of the red-edge transient absorption. The results of fitting for C_2 symmetric dyes were listed in our previous papers.[9,48] For D_3 symmetric dyes, three components, $\tau_1-\tau_3$, were necessary to fit the positive signal and one component, τ_{rise}, was necessary to fit the decay of the red-edge absorption. The fitting results are listed in Table 1 and Table 2. The viscosity dependences of the decay components are shown in Figure 11.

Both linear[32−34,40] and nonlinear[3,59,64,65] viscosity dependences have been reported for the excited state lifetime of TPM dyes. It is now generally accepted that in short linear alcohol solvents, the viscosity dependence is quite linear.[32−34,40] For each component of the multiexponential decay of the PP signals (Figure 11), linear viscosity dependence can be seen. Even the subpicosecond components showed viscosity dependence, except for τ_1 of MG. In the case of MG, τ_1 did not show viscosity dependence although its amplitude, A_1, decreased with increasing viscosity.[9,48] An interesting trend is that the viscosity dependences are stronger for slower dynamics, i.e., the slopes are steeper. This can be the effect of the time-dependent viscosity or the hierarchy structure of the solvation shell. In the ultrafast time regime, the twisting phenyl ring will first collide with a few solvent molecules in the first solvation shell. In later times, the phenyl ring will collide with more solvent molecules and the collided solvent molecules will also collide with other solvent molecules in the outer shell. Therefore, the microscopic viscosity becomes more macroscopic with increasing time.

We would like to mention that the aqueous solution deviates slightly from the viscosity-dependent slope obtained from *n*-alcohols. The viscosity of methanol is 0.61 cP at 20 °C, which is smaller than that of water, 1.00 cP. However, as can be seen in Figure 2, aqueous solution decays faster than methanol. The viscosity of D_2O is 1.248 cP, which causes slower decay than H_2O (Figure 4). The viscosity of ethanol is 1.19 cP, which is similar to that of D_2O. However, the decay time for the slowest component was 0.57 ps in D_2O, which is almost twice as short as that in ethanol, 1.0 ps. This is a good example of the effect of microscopic molecular nature being stronger than a bulk solvent property. The existence of alkyl chains seems to greatly reduce the rate of diffusive twisting of the phenyl ring.

The Arrhenius plots for MG and CV in ethanol are shown in Figure 13. The fastest component showed almost no temperature dependence. This result supports the idea of this component originating from a low frequency intramolecular mode or the inertial solvation and not from the diffusive rotation. An additional slow decay component was necessary to fit the decay of MG below 220 K. We have obtained an activation energy for each decay component by fitting the points above 180 K where the slope looks linear. The results are 290, 360, and 700 cm^{-1} for τ_{rise1}, τ_2, and τ_3 of MG, respectively, and 240 and 460 cm^{-1} for τ_2 and τ_3 of CV, respectively. The slower decay had larger activation energy. The deactivation process of TPM dyes is considered to be barrierless.[32−34] Thus, these activation energies must have originated completely from solvent properties. We have obtained the activation energy of the viscosity of ethanol from the Arrhenius plot shown in Figure 14. The activation energy for ethanol viscosity was 1060 cm^{-1}, which is much higher than any of the activation energy obtained from the decays of TPM dyes. This can be also understood in terms of the time-dependent viscosity or the hierarchy structure of the solvation shell. Since the twisting of the phenyl ring itself is barrierless and it collides only with a few solvent molecules in the earlier times, the activation energy will be small at the beginning. As the number of colliding solvent molecules increases with time, the activation energy will increase and approach the value of that of the bulk ethanol viscosity.

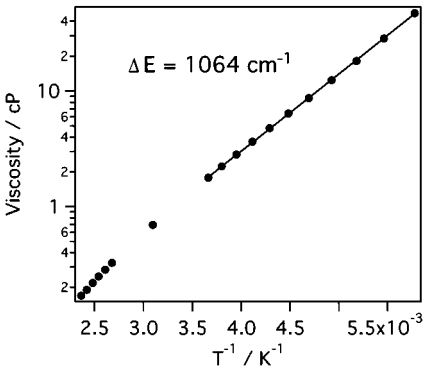

Figure 14. Arrhenius plot of the viscosity of ethanol. The values were taken from ref 67. A fitting below 273 K gives activation energy of 1064 cm^{-1}.

According to the Stokes−Einstein−Debye theory, rotational diffusion time depends on viscosity and temperature as

$$\tau_{rot} = \frac{V\eta}{K_B T} \tag{2}$$

where V is the effective volume and K_B is the Boltzmann constant. In Figure 15, time constants are plotted against η/T. From the slope of this figure, it can be seen that the slower decays have larger effective volumes. For CV in ethanol solution shown in Figure 15b, the effective volume for the τ_3 component is more than 6 times larger than that of τ_2 component. This can be also understood with the hierarchy structure of the solvation shell. As the number of colliding solvent molecules increases with time, the effective volume will also increase despite the constant volume of the actual phenyl ring.

Since all of the previously proposed theoretical models consider only a single diffusion constant, they are expected to fail to describe such complex aspects of the experimental observations. Another problem of these models is that they do not consider the effect of heating and cooling of the surrounding solvent molecules. It is assumed that the heat bath and the heat conduction are infinitively large and fast. Thus, the temperature of the system is always constant. However, in the real experimental system, heat conductivity is finite and the twisting can result in the heating of the solvation shell. Ultrafast reaction will be followed by the heating and the cooling of the solvation shell.

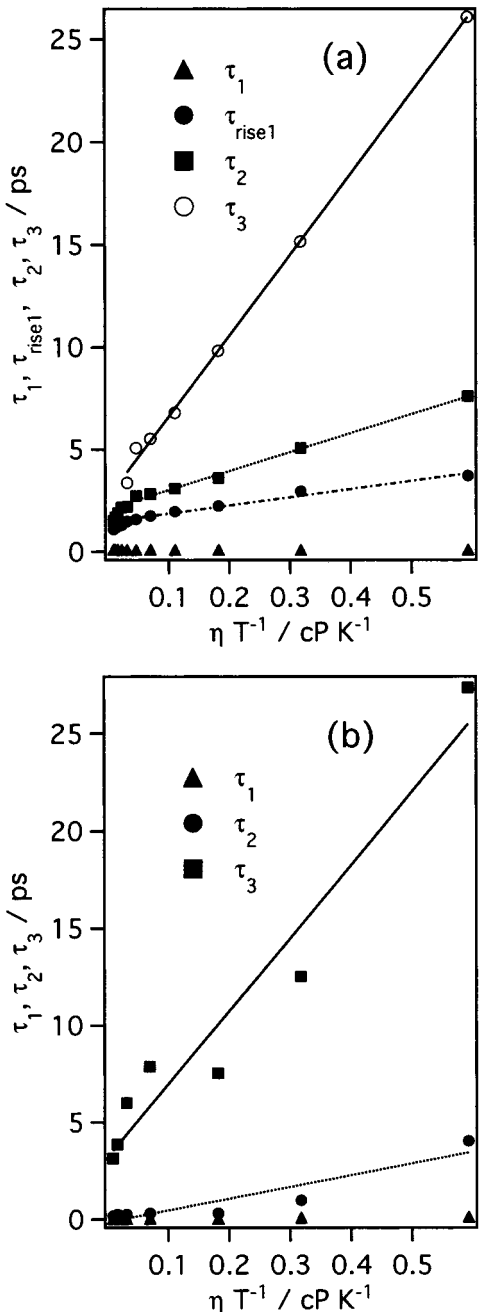

Figure 15. (a) Plots of the time constants τ_1, τ_{rise1}, τ_2, and τ_3 of MG in ethanol solution against η/T (▲, ●, ■, and ○, respectively). Fitting was carried out below 220 K and the slopes were 4.0, 9.3, and 39.5 for τ_{rise1}, τ_2, and τ_3, respectively. (b) Plots of the time constants τ_1, τ_2, and τ_3 of CV in ethanol solution against η/T (▲, ●, and ■, respectively). The slopes obtained from the fitting were 6.1 and 37.6 for τ_2 and τ_3, respectively.

5. Conclusions

We have carried out ultrafast pump−probe measurements of TPM dyes with a time resolution of 30 fs. The pump−probe signal showed that the solvent dependent nature of TMP dyes arose first in the femtosecond time regime, e.g., the decay of *n*-butanol solution was already slower than the methanol solution just 50 fs after the initial photoexcitation. This difference seems to have originated from the inertial motion of the solvent molecules. The signal decays in a multiexponential manner, and the slower components showed stronger linear dependence on the solvent viscosity than the faster ones. We have also carried out temperature-dependent measurement of ethanol solution and calculated the activation energies from the Arrhenius plots of each components. We found that the activation energy of the viscosity of ethanol was larger than that of any components of TPM dyes. The activation energies and effective volumes were larger for slower decays. These observations can be the effect of the time-dependent viscosity or the hierarchy structure of the solvation shell. In the ultrafast time regime, the twisting phenyl ring will first collide with a few solvent molecules in the first solvation shell. In later times, the phenyl ring will collide with more solvent molecules, and the collided solvent molecules will also collide with other solvent molecules in the outer shell. Therefore, the microscopic viscosity becomes more macroscopic with increasing time.

The lifetime of the transient absorption appearing at the red edge of the ground state absorption was longer than any of the reported lifetimes of the excited state absorptions around 400 nm. Therefore, the red-edge absorption was assigned to the unrelaxed ground state molecule with a distorted phenyl group. For CV in methanol, anisotropy showed an ultrafast decay of 110 fs, which indicates that not only the strength of the transition moment reduces but also the direction changes.

Finally, we would like to mention that recently a picosecond time-resolved X-ray diffraction measurement has been carried out on the crystal powder of the famous TICT molecule, *N*,*N*-dimethylaminobenzonitrile (DMABN).[66] The experiment revealed a twisting motion of the amino group up to 10 degrees within 80 ps. Application of such technique to the study of TPM dyes will be extremely enlightening.

Acknowledgment. This research was supported by a Grant-in-Aid for Specially Promoted Research (No. 10102007) from the Ministry of Education, Science, Sports, and Culture of Japan and also from the Sumitomo Foundation. Y.N. wishes to thank Mr. Bo Wegge Laursen for letting us know the information of tris(dialkylamino)-trioxatriangulenium dyes prior to the publication.

References and Notes

(1) Duxbury, D. F. *Chem. Rev.* **1993**, *93*, 381.
(2) Oster, G.; Nishijima, Y. *J. Am. Chem. Soc.* **1956**, *78*, 1581.
(3) Förster, T.; Hoffmann, G. *Z. Phys. Chem. NF* **1971**, *75*, 63.
(4) Martin, M. M.; Plaza, P.; Changenet, P.; Meyer, Y. H., *J. Photochem. Photobiol., A* **1997**, *105*, 197.
(5) Plaza, P.; Dai Hung, N.; Martin, M. M.; Meyer, Y. H.; Vogel, M.; Rettig, W. *Chem. Phys.* **1992**, *168*, 365.
(6) Laursen, B. W.; Krebs, F. C.; Nielson, M. F.; Bechgaard, K.; Christensen, J. B.; Harrit, N. *J. Am. Chem. Soc.* **1998**, *120*, 12255.
(7) Laursen, B. W., Thesis, University of Copenhagen, 2001.
(8) Laursen, B. W.; Reynisson, J.; Brinck, V.; Bechgaard, K.; Harrit, N., manuscript in preparation.
(9) Nagasawa, Y.; Ando, Y.; Okada, T. *Chem. Phys. Lett.* **1999**, *312*, 161.
(10) Mokhtari, A.; Fini, L.; Chesnoy, J. *J. Chem. Phys.* **1987**, *87*, 3429.
(11) Mokhtari, A.; Chesnoy, J. *Europhys. Lett.* **1988**, *5*, 523.
(12) Rosker, M. J.; Wise, F. W.; Tang, C. L. *Phys. Rev. Lett.* **1986**, *57*, 321.
(13) Angeloni, L.; Smulevich, G.; Marzocchi, M. P., *J. Raman Spectrosc.* **1979**, *8*, 305.
(14) Aleksandrov, I. V.; Bobovich, Y. S.; Vartanyan, A. T.; Sidorov, A. N. *Opt. Spectrosc.* **1977**, *42*, 35.
(15) Nelson, K. A.; Williams, L. R. *Phys. Rev. Lett.* **1987**, *58*, 745.
(16) Jurczok, M.; Plaza, P.; Martin, M. M.; Rettig, W. *J. Phys. Chem. A* **1999**, *103*, 3372.
(17) Martin, M. M.; Breheret, E.; Nesa, F.; Meyer, Y. H. *Chem. Phys.* **1989**, *130*, 279.
(18) Martin, M. M.; Plaza, P.; Meyer, Y. H. *J. Chem. Phys.* **1991**, *95*, 9310.
(19) Martin, M. M.; Plaza, P.; Meyer, Y. H. *Chem. Phys.* **1991**, *153*, 297.
(20) Ishikawa, M.; Ye, J. Y.; Maruyama, Y.; Nakatsuka, H., *J. Phys. Chem. A* **1999**, *103*, 4319.
(21) Ishikawa, M.; Maruyama, Y. *Chem. Phys. Lett.* **1994**, *219*, 416.

(22) Maruyama, Y.; Ishikawa, M.; Satozono, H. *J. Am. Chem. Soc.* **1996**, *118*, 6257.
(23) Maruyama, Y.; Magnin, O.; Satozono, H.; Ishikawa, M. *J. Phys. Chem. A* **1999**, *103*, 5629.
(24) Migus, A.; Etchepare, J.; Grillon, G.; Thomazeau, I.; Antonetti, A. *J. Opt. Soc. Am. B* **1984**, *1*, 454.
(25) Ben-Amotz, D.; Harris, C. B. *Chem. Phys. Lett.* **1985**, *119*, 305.
(26) Vogel, M.; Rettig, W. *Ber. Bunsen-Ges. Phys. Chem.* **1985**, *89*, 962.
(27) Vogel, M.; Rettig, W. *Ber. Bunsen-Ges. Phys. Chem.* **1987**, *91*, 1241.
(28) Sundström, V.; Gillbro, T.; Bergström, H. *Chem. Phys.* **1982**, *73*, 439.
(29) Robl, T.; Seilmeier, A. *Chem. Phys. Lett.* **1988**, *147*, 544.
(30) Bagchi, B.; Fleming, G. R.; Oxtoby, D. W. *J. Chem. Phys.* **1983**, *78*, 7375.
(31) Bagchi, B.; Fleming, G. R.; Oxtoby, D. W. *Chem. Phys. Lett.* **1983**, *99*, 225.
(32) Ben-Amotz, D.; Jeanloz, R.; Harris, C. B. *J. Chem. Phys.* **1987**, *86*, 6119.
(33) Ben-Amotz, D.; Harris, C. B. *J. Chem. Phys.* **1987**, *86*, 4856.
(34) Ben-Amotz, D.; Harris, C. B. *J. Chem. Phys.* **1987**, *86*, 5433.
(35) Nagasawa, Y.; Ando, Y.; Watanabe, Y.; Okada, T. *App. Phys. B [Suppl.]* **2000**, *70*, S33.
(36) Miyasaka, H.; Murakami, M.; Irie, A., in preparation.
(37) Lewis, G. N.; Magel, T. T.; Lipkin, D. *J. Am. Chem. Soc.* **1942**, *64*, 1774.
(38) Loony, C. W.; Simpson, W. T. *J. Am. Chem. Soc.* **1954**, *76*, 6293.
(39) Adam, F. C.; Simpson, W. T. *J. Mol. Spectrosc.* **1959**, *3*, 363.
(40) Sundström, V.; Gillbro, T. *J. Chem. Phys.* **1984**, *81*, 3463.
(41) Clark, F. T.; Drickamer, H. G. *J. Phys. Chem.* **1986**, *90*, 589.
(42) Clark, F. T.; Drickamer, H. G. *J. Chem. Phys.* **1984**, *81*, 1024.
(43) Korppi-Tommola, J.; Yip, R. W. *Can. J. Chem.* **1981**, *59*, 191.
(44) Korppi-Tommola, J.; Kolemainen, E.; Salo, E. *Chem. Phys. Lett.* **1984**, *104*, 373.
(45) Lovell, S.; Marquardt, B. J.; Kahr, B., *J. Chem. Soc., Perkin Trans.* **1999**, *2*, 2241.
(46) Lueck, H. B.; McHale, J. L.; Edwards, W. D. *J. Am. Chem. Soc.* **1992**, *114*, 2342.
(47) Lueck, H. B.; Rice, B. L.; McHale, J. L. *Spectrochim. Acta* **1992**, *48A*, 819.
(48) Nagasawa, Y.; Ando, Y.; Okada, T. *J. Chin. Chem. Soc.* **2000**, *47*, 699.
(49) Lueck, H. B.; Daniel, D. C.; McHale, J. L. *J. Raman Spectrosc.* **1993**, *24*, 363.
(50) Sunder, S.; Bernstein, H. J. *Can. J. Chem.* **1981**, *59*, 964.
(51) Walmsley, I. A.; Wise, F. W.; Tang, C. L. *Chem. Phys. Lett.* **1989**, *154*, 315.
(52) Yang, T.-S.; Chang, M.-S.; Chang, R.; Hayashi, M.; Lin, S. H.; Vöringer, P.; Dietz, W.; Scherer, N. F. *J. Chem. Phys.* **1999**, *110*, 12070.
(53) Jimenez, R.; Fleming, G. R.; Kumar, P. V.; Maroncelli, M. *Nature* **1994**, *369*, 471.
(54) Rosenthal, S. J.; Xie, X.; Du, M.; Fleming, G. R. *J. Chem. Phys.* **1991**, *95*, 4715.
(55) Bardeen, C. J.; Rosenthal, S. J.; Shank, C. V. *J. Phys. Chem. A* **1999**, *103*, 10506.
(56) Bardeen, C. J.; Shank, C. V. *Chem. Phys. Lett.* **1994**, *226*, 310.
(57) Du, M.; Jia, Y.; Fleming, G. R. In *Ultrafast Phenomena IX*; Barbara, P. F., Knox, W. H., Mourou, G. A., Zewail, A. H.; Springer-Verlag: Berlin, 1994; p 515.
(58) Jonas, D. M.; Fleming, G. R. In *Ultrafast processes in photochemistry and photobiology*; Blackwell Scientific: Oxford, 1995; p 225.
(59) Yoshizawa, M.; Suzuki, K.; Kubo, A.; Saikan, S. *Chem. Phys. Lett.* **1998**, *290*, 43.
(60) van der Meer, M. J.; Zhang, H.; Glasbeek, M. *J. Chem. Phys.* **2000**, *112*, 2878.
(61) Changenet, P.; Zhang, H.; van der Meer, M. J.; Glasbeek, M.; Plaza, P.; Martin, M. M. *J. Phys. Chem. A* **1998**, *102*, 6716.
(62) Iwata, K.; Hamaguchi, H. *J. Phys. Chem. A* **1997**, *101*, 632.
(63) Cremers, D. A.; Windsor, M. W. *Chem. Phys. Lett.* **1980**, *71*, 27.
(64) Madge, D.; Windsor, M. W. *Chem. Phys. Lett.* **1974**, *24*, 144.
(65) Ippen, E. P.; Shank, C. V.; Bergman, A. *Chem. Phys. Lett.* **1976**, *38*, 611.
(66) Techert, S.; Schotte, F.; Wulff, M. *Phys. Rev. Lett.* **2001**, *86*, 2030.
(67) Kutateladze, S. S.; Borishanskii, V. M. *A concise encyclopedia of heat transfer*, first English edition; Pergaman Press: London, 1966.